Nuclear Instruments and Methods in Physics Research A 1065 (2024) 169518

Contents lists available at ScienceDirect

Nuclear Inst. and Methods in Physics Research, A

journal homepage: www.elsevier.com/locate/nima

INSPIRE: Challenge of 50 kg-class satellite to open up MeV gamma-ray astronomy

J. Kataoka [a,*], R. Iwashita [a], K.S. Tanaka [a], R. Mori [a], S. Ogasawara [a], T. Suga [a], N. Koshikawa [a], K. Watanabe [b], M. Yasuda [b], H. Kobayashi [b], D. Kobayashi [b], K. Otsubo [b], A. Ohira [b], Y. Amaki [b], Y. Arai [b], K. Tashiro [b], Y. Ozeki [b], Y. Kawaguchi [b], D. Yoshimura [b], H. Yoshida [b], K. Takahashi [b], Y. Yatsu [b], T. Chujo [b], H. Nakanishi [b], M. Onishi [c], S. Takeda [c]

[a] Faculty of Science and Engineering, Waseda University, 3-4-1 Okubo, Shinjuku-ku, Tokyo, 169-8555, Japan
[b] Tokyo Institute of Technology, 2-12-1 Ookayama, Meguro-ku, Tokyo, 152-8550, Japan
[c] iMAGINE-X Inc., 1-12-8 Shibuya, Shibuya-ku, Tokyo, 150-0002, Japan

ARTICLE INFO

Keywords:
Small satellite
MeV gamma rays
Neutron capture
Compton camera
Kilonova

ABSTRACT

Waseda University and Tokyo Tech are developing a 50 kg-class small satellite, tentatively named INnovative Space Probe for Imaging R-process Emission (*INSPIRE*), which is scheduled for launch in 2027. The primary detector of the satellite is a BOX-type Compton Camera (CC-Box) that enables to observe low energy gamma rays (30 keV–200 keV) in pinhole mode and high energy gamma rays (150 keV–3 MeV) in Compton mode. The CC-Box consists of a pixelized Ce:GAGG scintillator array using a depth-of-interaction (DOI) structure, which is optically coupled to an MPPC array. The Ce:GAGG arrays are also positioned on the side of detector to enhance its sensitivity. Herein, we describe the detailed design of the CC-Box, its data processing flow, and its weight and power specifications. We then assess the anticipated performance of the detector in terms of continuum and line sensitivities, together with a simulation of the Crab nebula observation. Finally, a brief review of the experimental results is performed using hands-on devices already implemented in nuclear medicine and atmospheric observations, such as gamma-ray imaging of thunderclouds.

1. Introduction

Approximately 300 stable elements exist in nature, ranging from hydrogen ($^{1}_{1}$H) to the heaviest, uranium ($^{238}_{92}$U). Most of elements heavier than iron ($^{56}_{26}$Fe), are thought to be produced by neutron capture (NC; $^{A}_{Z}X + n \rightarrow {}^{A+1}_{Z}X$, where X is the element of interest) through the so-called *s*-process [1]. However, many other elements have unknown origins. In particular, the origin of Pt, Au and various rare-earth elements is still under debate; according to numerical simulations, they may have originated in an explosive event such as binary neutron star mergers called "kilonova" through the *r*-process. The recent detection of GW170817/At1017gfo confirmed the existence of *r*-process elements in kilonova [2,3].

Gamma rays in the range of MeV are one of the best probes for understanding nucleosynthesis in the universe, as most unstable elements emit specific gamma rays corresponding to *Q*-value in nuclear reactions. In NC, unstable elements falls to their ground state through β-decay and emit gamma rays ranging from a few tens of keV to more than MeV. In the case of kilonova, 20–50% of the total radioactive energy can be released in the form of gamma rays on timescales of hours to a month; therefore, a number of gamma-ray lines are anticipated in the spectra between 30 keV and 3 MeV [4,5].

However, MeV observations in space are difficult for several reasons. First, gamma rays cannot be focused with lenses or reflection mirrors; therefore, other imaging techniques, such as pinhole cameras [6] and coded aperture masks [7], are necessary. Using a Compton camera should be considered for the MeV range [8]. Second, the isotropic gamma-ray background severely contaminates the observed spectrum. In the 1990's, COMPTEL/*CGRO* provided a 1 to 30 MeV all-sky map [9] after the discovery of 1.809 MeV gamma rays emitted from ^{26}Al along the Galactic plane [10]. In the 2000's, the SPI/*INTEGRAL* provided an improved map and spectra of various line emissions using a coded aperture mask [11]. However, the mass of COMPTEL and SPI exceeded 1000 kg, which prevented successors in MeV gamma-ray astronomy.

In this context, more than 300 small satellites are launched worldwide annually, some of which are used to promote space science. In

* Corresponding author.
E-mail address: kataoka.jun@waseda.jp (J. Kataoka).

https://doi.org/10.1016/j.nima.2024.169518
Received 9 January 2024; Received in revised form 29 May 2024; Accepted 8 June 2024
Available online 10 June 2024

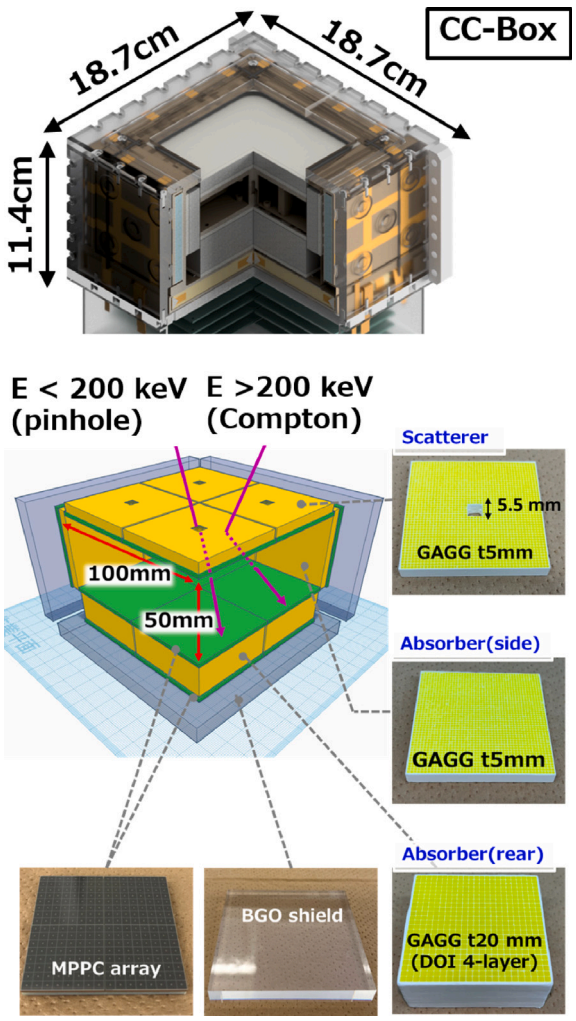

Fig. 1. Schematic design (*upper*) and detector components of the CC-Box (*bottom*).

Japan, Tokyo Tech successfully launched a $50 \times 50 \times 50$ cm^3 and 50 kg-class satellite, *HIBARI*, in 2021, and second satellite, *PETREL*, is planned for launch in 2024 [12]. *PETREL* has an ultra-violet (UV) telescope as the main detector to detect shock breakouts associated with kilonovae. Along with these missions, INnovative Space Probe for Imaging R-process Emission (*INSPIRE*) is the third mission dedicated to MeV gamma-ray astronomy using a 50 kg-class satellite. In this study, we present a detailed design of detectors, as well as the expected performance and experimental results using hands-on devices already implemented in nuclear medicine and atmospheric gamma-ray observations.

2. Mission concept

2.1. Design of CC-Box

Fig. 1 shows the overall design of the Compton camera box (CC-Box) onboard *INSPIRE*. The CC-Box can simultaneously observe low-energy gamma ray (30–200 keV) in the pinhole mode and high-energy gamma rays (200 keV–3 MeV) in the Compton mode [13,14]. It has a 2×2 array of sensor elements, which comprise a pixelized Ce:GAGG scintillator array of 5×5 cm^2 optically coupled with a 16×16ch MPPC array. The Ce:GAGG scatter layer is 5 mm thick with a 5×5 mm^2 pinhole in the center. The absorber features a four-layer, 20 mm-thick depth-of-interaction (DOI) structure. The pixel size of Ce:GAGG is 1×1 mm^2 for the scatterer, whereas 2×2 mm^2 for absorber. Peripheral Ce:GAGG elements were positioned as side absorbers to enhance the sensitivity. Furthermore, BGO shields surround the side and bottom of the detector not only for efficient background rejection but also to identify escape events in which incident gamma rays cannot be completely absorbed within Ce:GAGG elements [15]. Each BGO shield was read out using a monolithic 6×6 mm^2 MPPC. The total weight of CC-Box is 10 kg.

2.2. Data processing

Each 16×16 ch MPPC array was read out through a resistive-chain network to reduce the number of channels. As shown in Fig. 2, Ce:GAGG elements output 80 anode signals, and BGO active shields output 12 anode signals. All these signals are fed into six analog boards that have 16-ch filter amplifiers, peak-hold LSIs, and a 12-bit ADC. Moreover, each analog board has four HV modules to control the MPPC gain against the temperature variations. The pulse-height data from each analog board are formatted and transferred to the USB board by adding timestamp and header information. Finally, the Raspberry PI controls the data handling and command operation between the CC-Box and satellite instruments, such as the science handling unit (SHU) and command handling unit (CHU-F), through an interface module (CAM-main). The maximum event rate that can be acquired with the CC-Box is 80 kcps. The total power required for the CC-Box, including analog, USB boards and Raspberry PI, is 18 W for full operation.

3. Performance

3.1. Angular resolution and intrinsic efficiency

The two most important characteristics of gamma-ray camera are (1) angular resolution ($\Delta\theta$), and (2) intrinsic efficiency (η). Fig. 3(a) shows the angular resolution of the pinhole and Compton images as a function of energy, where the angular resolution measure (ARM) was plotted for the Compton imaging. The $\Delta\theta$ of the CC-Box is almost equal to or higher than that of COMPTEL between 30 keV and 3 MeV. Fig. 3(b) shows the intrinsic detection efficiency η, which indicates the fraction of events detected for all the radiation emitted towards the detector. Again, the η of CC-Box is higher than that of COMPTEL below 1.3 MeV in the Compton mode.

3.2. Continuum and line sensitivities

Fig. 4 shows the anticipated performance of *INSPIRE* in terms of the continuum (S_C) and line sensitivities (S_L). The sensitivities were derived as follows:

$$S_C(E) = \frac{f}{\eta(E)}\sqrt{\frac{b(E)}{A\Delta E T}}, \quad (1)$$

$$S_L(E) = \frac{f}{\eta(E)}\sqrt{\frac{2b(E)\delta E}{AT}}, \quad (2)$$

where, $\eta(E)$ is the intrinsic efficiency, as shown in Fig. 3(b), and $b(E)$ is the background, which is primarily affected by the Cosmic X-ray background (CXB) and albedo gamma rays [16]. $A = 100$ cm^2 is the geometrical area of the CC-Box, and T is the observation time in seconds. ΔE is the energy window for continuum emission, which was fixed as $E = \Delta E$, and $\delta E = 7.3\times(E[\mathrm{MeV}])^{-1/2}$ % (FWHM; Full Width at Half Maximum) is the energy resolution for line emission. f is the detection significance and was set as $f = 3$. The CC-Box can extend the observation window to 30 keV; however, the S_C sharply degrades owing to the severe contamination of albedo gamma rays above the MeV range. The line sensitivity S_L is comparable to or better than that of COMPTEL below 2 MeV in the Compton mode. In addition, S_L is comparable to that of *COSI* [17] below 500 keV. *COSI* is NASA's Small Explorers (SMEX) Mission, also planned for launch around 2027, with a total mass of 400 kg.

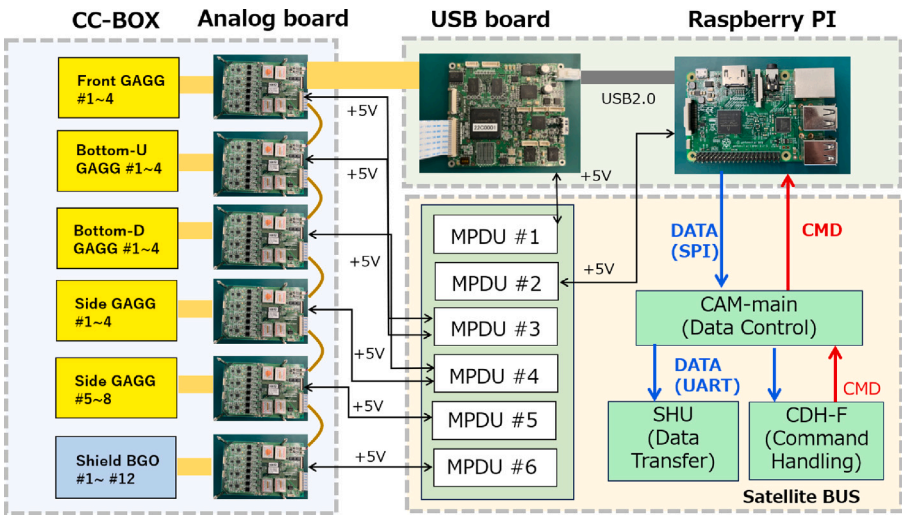

Fig. 2. Overview of the data acquisition system onboard *INSPIRE*.

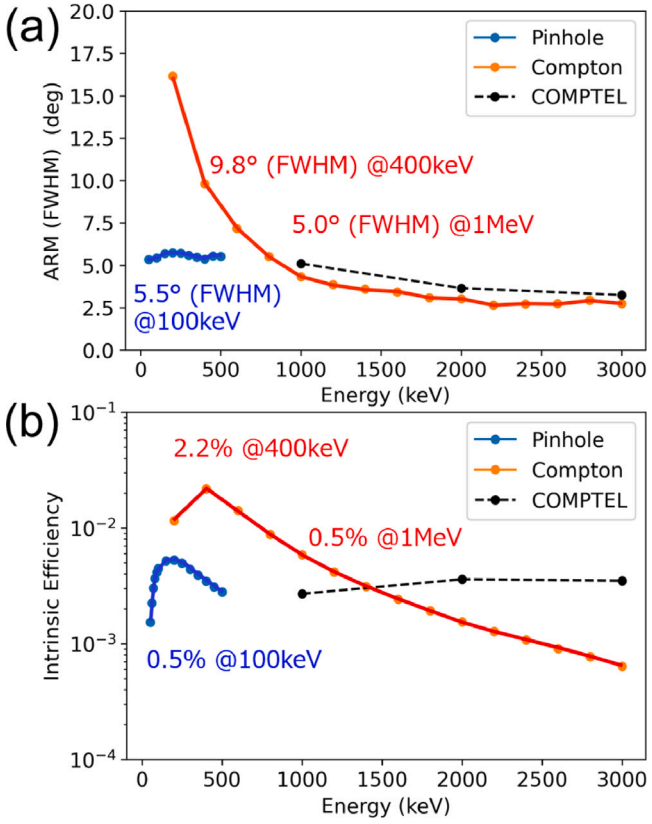

Fig. 3. Simulated performance of the CC-Box between 30 keV and 3 MeV. (a) Angular resolution and (b) intrinsic efficiency.

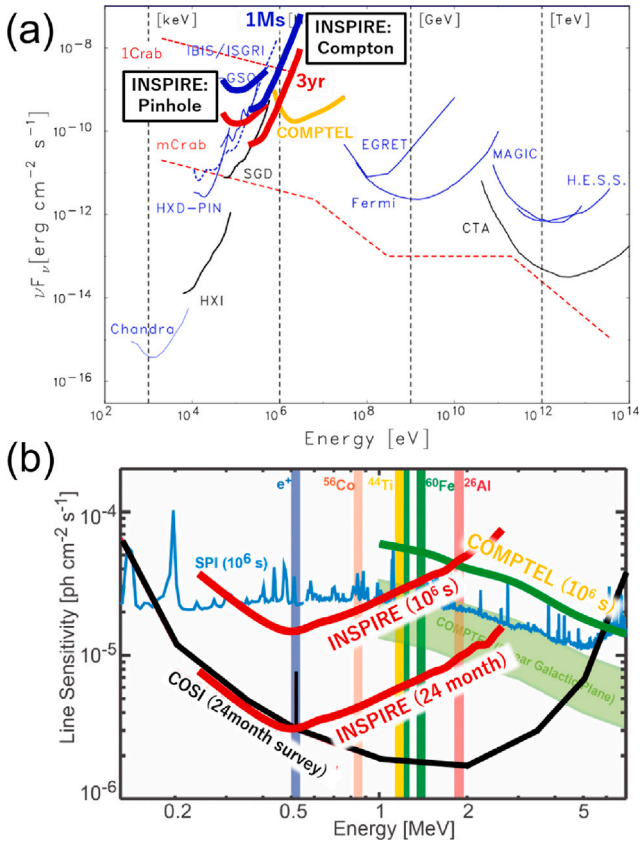

Fig. 4. Anticipated sensitivity of *INSPIRE* compared to other missions. (a) Continuum sensitivity and (b) line sensitivity.
Source: The figures are reconstructed from [17,18].

3.3. Simulation of Crab nebula

Fig. 5(a: *left*) compares the Crab nebula spectrum and dominant background assuming a Sun-synchronous orbit (SSO). The CXB ($\propto E^{-2.9}$; shown in *red*) dominated the background below 150 keV, while albedo gamma rays ($\propto E^{-1.4}$; shown in *green*) became more significant above 150 keV. Even for a bright source like the Crab nebula ($\propto E^{-2.2}$; shown in *black*), the anticipated flux was two order of magnitude lower than the background. However, as shown in Fig. 5(a: *right*), *INSPIRE* could detect the Crab nebula with more than $\simeq$30 σ significance when reconstructing a Compton image between 300 keV and 1.5 MeV for a 10^6 sec observation.

3.4. Other targets

While the primary target of observation for *INPSIRE* is kilonovae, detectable events rarely occur during mission life of typically a several years [5]. Therefore, we also plan deep scans of the Galactic plane, as performed by COMPTEL/*CGRO* and SPI/*INTEGRAL*. Moreover,

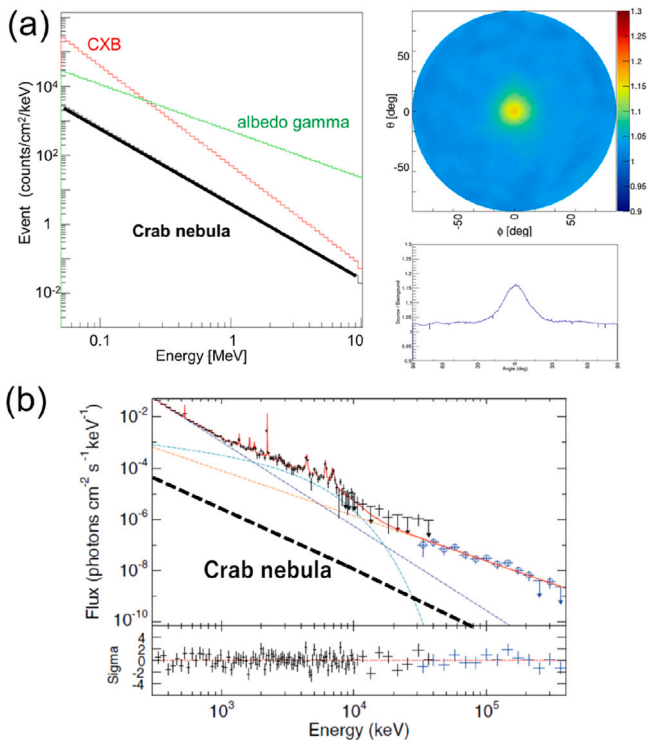

Fig. 5. (a)*left*: Background (CXB: *red*, albedo gamma: *green*) assuming a Sun-synchronous orbit as compared to the Crab nebula spectrum (*black*). *right*: Simulated Crab image obtained with *INSPIRE* assuming a 10^6 sec observation. (b) Comparison between the Crab nebula spectrum and typical M-class solar flare.
Source: The figure is reconstructed from [19].

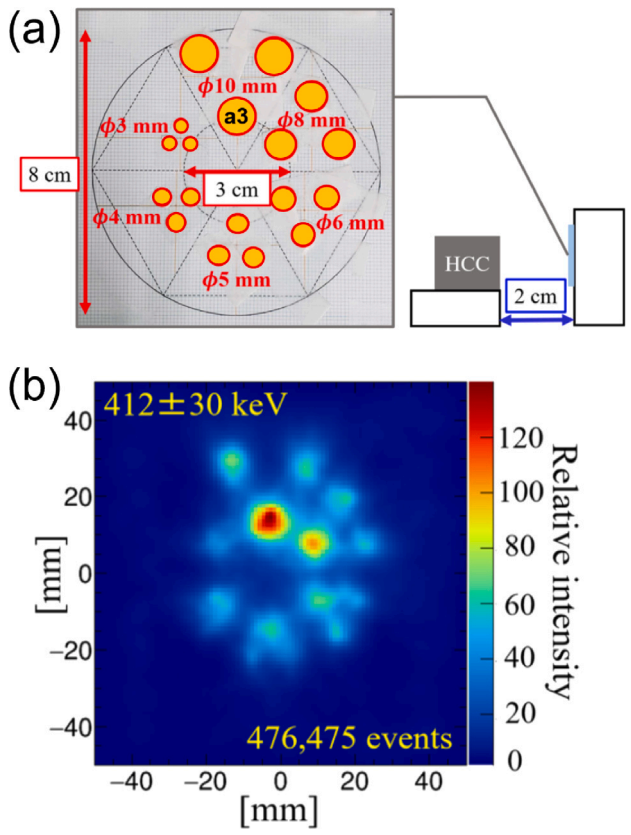

Fig. 6. Activating gold plates using thermal neutrons to mimic the NC process in kilonova. (a) Setup and placement geometry of each gold plates arranged in Derenzo phantom. (b) The image of activated golds with 412 keV gamma rays.

transient events such as AGN flares, gamma-ray bursts, and solar flares are potential targets. Particularly in the solar maximum around 2027, 200–300 solar flares having a flux greater than 10^{-5} W/m^2 ("M-class" flares) are expected annually [19]. As shown in Fig. 5(b), the gamma-ray flux of an M-class flare was two orders of magnitude higher than that of the Crab nebula. In such cases, various gamma-ray lines, if present, could be easily detected using *INSPIRE*.

4. Experiments using hands-on devices

4.1. Activation imaging: NC of ^{197}Au

In parallel with abovementioned detailed simulations, we have developed various hands-on devices as a prototype sensor of the CC-Box. The first example is the performance testing of a pinhole/Compton camera (a hybrid Compton camera;[13]) of 5 × 5 cm^2, which is quarter the size of the CC-Box. To mimic the phenomenon of NC that occurs in kilonovae, we irradiated stable gold (^{197}Au) using thermal neutrons. This concept is also used for drug visualization in animals and humans [20]. Activated gold emits 412 keV gamma rays through the NC of $^{197}_{79}\mathrm{Au} + n \rightarrow {}^{198}_{79}\mathrm{Au} \rightarrow {}^{198}_{80}\mathrm{Hg} + e^- + \gamma$ with a half-life time of $\tau_{1/2} = 2.7$ day. Fig. 6 shows an example image of 412 keV gamma rays from various Au plate sizes [21]. The distance between the camera and phantom was 20 mm, and the intensity of the strongest plate (a3) was approximately 13.0 kBq, with a 16 h measurement time.

4.2. Quasi-monochromatic MeV gamma-ray imaging

To test the gamma-ray imaging performance at energies greater than MeV, we installed a Compton camera that has two scatterer layers and a 3D position-sensitive absorber. Each scatterer comprise 42 × 42 arrays of 0.5×0.5×3.0 mm^3 Ce:GAGG cubes, whereas 22 × 22 × 10 arrays of 2.0 × 2.0 × 4.0 mm^3 Ce:GAGG cubes were used as an absorber [22]. We tested the detector at NewSUBARU, which provides a quasi-monochromatic MeV gamma-ray beam through inverse Compton scattering of a CO_2 laser with 1 or 1.5 GeV electrons. Fig. 7 shows an example image of 1.7 MeV gamma-ray beams irradiated from 0° and 20° off the Compton camera axis. The ARM obtained was 3.4 ± 0.1° (FWHM) at 1.7 MeV and 4.0 ± 0.5° (FWHM) at 3.9 MeV, which was almost equal to the expected performance of the CC-Box onboard *INSPIRE*.

4.3. Gamma-ray imaging of a thundercloud

To demonstrate the imaging performance of the Compton camera for continuum emissions, we observed thunderclouds. In January 2022, we detected a gamma-ray glow lasting 4 min in a mountainous area 25 km from the Japan Sea and 410 m above sea level. Fig. 8 shows the observed light curve and the image obtained using a Compton camera [23]. The observed spectrum exhibited a flat power-law shape of $\propto E^{-1.0}$. The overall dimensions of the Compton camera were 10 × 10 cm^2; therefore, they were almost the same as those of the CC-Box in *INSPIRE*. The observed image indicated two enhanced concentrations at 4.0 and 5.9 σ levels in a range of 0.15–1.5 MeV. Notably, this is the first case of direct imaging of gamma rays from thunderclouds.

5. Conclusion

We are developing a 50 kg-class small satellite, *INSPIRE*, planned for launch in 2027. The main onboard detector is the CC-Box, which can image gamma rays from 30 keV to 3 MeV by combining pinhole and

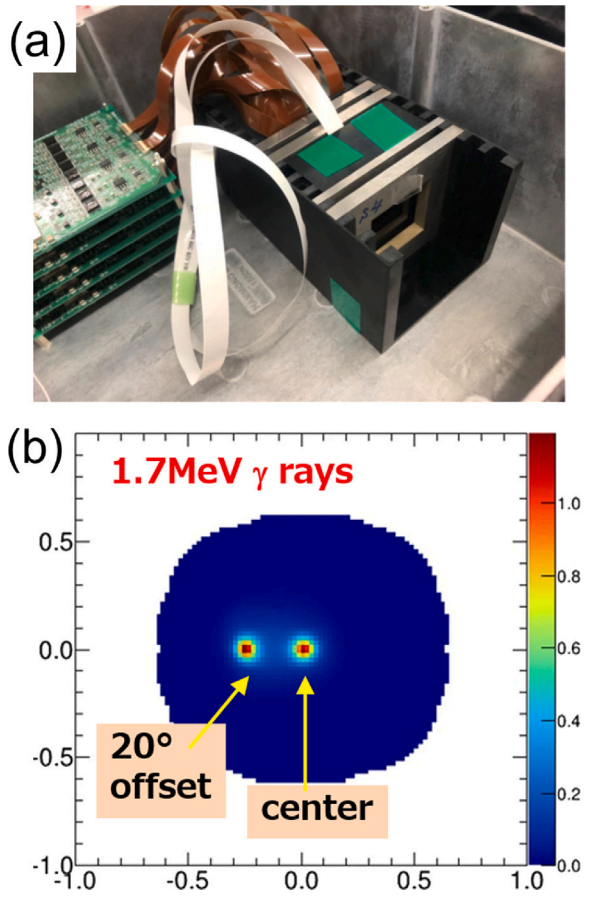

Fig. 7. (a) 3D position-sensitive Compton camera that features imaging of high energy gamma rays above MeV. (b) An example image of a quasi-monochromatic 1.7 MeV gamma-ray from the on-set and off-set directions, as measured in NewSubaru. The color scale of the right side indicates a relative intensity.

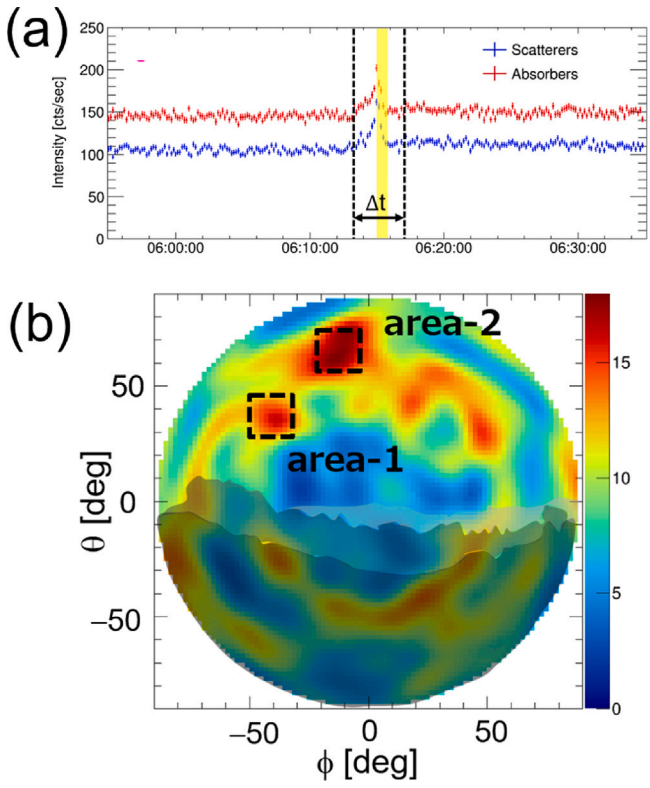

Fig. 8. (a) Temporal variations of gamma-ray flux as measured with Compton camera (*blue*: scatterer, *red*: absorber) during the glow observed in January 2022. (b) Gamma-ray image obtained with 10 × 10 cm^2 Compton camera. The energy range for image reconstruction was 150 keV–1 MeV. The color scale of the right side indicates a relative intensity.

Compton modes of observation. A prominent advantage of using small satellite mission is the possibility of quick and low-cost development with much more frequent launch opportunities compared to previous astronomical satellites weighting over 1000 kg. However, the resources are highly limited in terms of power, weight, size. In fact, the geometrical size of the CC-Box is just 18.7 × 18.7 cm^2. Nevertheless, it is expected to provide excellent performance in terms of both continuum and line sensitivities owing to the use of finely pixelized Ce:GAGG scintillator coupled with large-area MPPC arrays. Although the project is still in the initial phase of development, various simulation and experimental tests using hands-on devices suggest that *INSPIRE* can be a novel approach for MeV gamma-ray astronomy in the late 2020's.

Declaration of competing interest

The authors declare that they have no known competing financial interests or personal relationships that could have appeared to influence the work reported in this paper.

Acknowledgments

This research was supported by Japan Science and Technology Agency (JST) ERATO Grant Number JPMJER2102, Japan. We thank Dr. T. Mizuno for his useful comments and advices for simulation of CXB and albedo-gamma rays.

References

[1] A. Arcones, F. Thielemann, Astron. Astrophys. Rev. 31 (2023) 1.
[2] D. Watson, C.J. Hansen, J. Selsing, et al., Nature 574 (2019) 497.
[3] N. Domoto, M. Tanaka, S. Wanajo, K. Kawaguchi, Astrophys. J. 913 (2021) 26.
[4] K. Hotokezaka, S. Wanajo, M. Tanaka, et al., Mon. Not. R. Astron. Soc. 459 (2016) 35.
[5] Y. Terada, Y. Miwa, H. Ohsumi, et al., Astrophys. J. 933 (2022) 111.
[6] F.J. Beekman, F. van der Have, Eur. J. Nucl. Med. Mol. Imaging 34 (2007) 151.
[7] J.G. Ables, Publ. Astron. Soc. Aust. 1 (1968) 172.
[8] V. Schoenfelder, A. Himer, K. Schneider, Nucl. Instrum. Methods 107 (1973) 385.
[9] V. Schoenfelder, K. Bennett, J.J. Blom, et al., Astron. Astrophys. Suppl. Ser. 143 (2000) 145.
[10] U. Oberlack, K. Bennett, H. Bloemen, et al., Astron. Astrophys. Suppl. Ser. 120 (1996) 311.
[11] R. Diehl, H. Halloin, K. Kretschmer, et al., Nature 439 (2006) 45.
[12] K. Watanabe, H. Kobayashi, Y. Amaki, et al., JESA (2024) in press.
[13] A. Omata, J. Kataoka, K. Fujieda, et al., Sci. Rep. 10 (2020) 14064.
[14] A. Omata, M. Masubuchi, N. Koshikawa, et al., Sci. Rep. 12 (2022) 2546.
[15] M. Masubuchi, A. Omata, N. Koshikawa, et al., NIM-A 1045 (2023) 167581.
[16] T. Mizuno, T. Kamae, G. Godfrey, et al., Astrophys. J. 614 (2004) 1113.
[17] J. Tomstic, on behald of COSI collaboration, Proc. Sci. ICRC 2021 (2021).
[18] T. Takahashi, K. Mitsuda, R. Kelly, et al., Proc. SPIE 843 (2012) 84431Z.
[19] M. Ackermann, M. Ajello, A. Allafort, et al., Astrophys. J. 745 (2012) 144.
[20] N. Koshikawa, A. Omata, M. Masubuchi, et al., Appl. Phys. Lett. 121 (2022) 193701.
[21] N. Koshikawa, et al., 2024, in preparation.
[22] H. Hosokoshi, J. Kataoka, S. Mochizuki, et al., Sci. Rep. 9 (2019) 18551.
[23] E. Kuriyama, M. Masubuchi, N. Koshikawa, et al., Geophys. Res. Lett. 49 (2022) e2022GL100139.